AMONET: A Method for Detecting and Mitigating the Data Rate Degradation due to Interference Over Wireless Networks

Guohao Lan, Sangyup Han, Il-Gu Lee, and Myungchul Kim
School of Computing, KAIST, Daejeon, Republic of Korea
{guohao, ilu8318, iglee9, mck}@kaist.ac.kr

Abstract—Recently, wireless networking technologies have been evolving to support wider bandwidth, and longer radio range in denser networks. Therefore, there is a high probability that two or more networks will overlap and result in more co-channel interferences. To mitigate the interference, the centralized network system is a promising solution which is based on the conflicts information provided by the interference detection methods. However, in this paper, we reveal that the existing Passive Interference Detection method (PIE) is not accurate and may cause dramatic throughput decrease in dynamically interfered networks because it is based on a single data rate criterion. Moreover, we propose and implement AMONET, which is a centralized detection method considering the data rate degradation due to interference (DRDI). Our simulation results demonstrate that the proposed scheme can improve aggregate throughput by 2.68x gains in the interfered wireless links over distributed coordination function (DCF), while PIE achieves 1.8x gains over DCF.

I. Introduction

Within the last decades, we have witnessed the rapid growth of the IEEE 802.11 based wireless networks, as known as Wi-Fi. According to a recent report [1], in the year of 2018, the Wi-Fi traffic will account for 61 percent of the IP traffic and 76 percent of the Internet traffic. This trend of traffic growth results from the increase of mobile station (MS) and the dense deployment of Wi-Fi Access Point (AP). And we can expect that, the current Wi-Fi networks are becoming denser. Unfortunately, due to the limited number of available Wi-Fi channels, a dense network will cause more co-channel interference and result in lower system throughput [2].

To optimize the performance of the Wi-Fi networks, many works have been proposed, such as utilizing multiple antennas [10], [11], controlling transmit power to adjust the interference range of mobile stations [3], [4], applying channel assignment to mitigate the co-channel interference between adjacent APs [5], [6], or using centralized system to schedule packet transmissions [7]–[9]. Other than the adoption of multiple antennas, the other works assume the existence of an accurate data structure which provides the information of interference relations between links in the wireless network. Such a data structure is known as the Conflict Graph (CG) [13]. In the literature, methods for building the conflict graph for a given

wireless network can be briefly classified into either active or passive methods. Active interference estimation methods such as, the Interference maps [14] and Micro-probing [15] use active probing to infer the interference relation. Although such approaches are accurate in identifying the interference, their measurement and computing overheads are large when they are applied to a network containing a large number of links. In addition, active methods can hardly be efficient in dynamic environment, in which the network topology changes frequently [16].

On the other hand, the passive methods infer the interference relation mainly based on the passively collected packet traces (either using the off-line packet traces [17], or using on-line monitoring data [16]). Although passive methods have been proven to be efficient to create the conflict graph, they are not accurate in detecting the Data Rate Degradation due to Interference (DRDI), which forces a victim wireless link to degrade its transmission data rate to endure the interference. For instance, the Passive Interference Estimation (PIE) [16] infers the links' interference relation by using the Link Interference Ratio (LIR) [18] at a single data rate only. However, current Wi-Fi networks provide various Modulation and Coding Schemes (MCSs) to enable the trade-off between the transmission efficiency and link reliability. While a high data rate is more efficient in data transmission, a low data rate is more robust against channel noise and co-channel interference. Accordingly, APs can apply the data rate adaptation algorithm [19] to adjust the link's transmission data rate depending on the interference level. When a link is suffering the DRDI, though no packets can be successfully delivered at a high data rate, it can still maintain a high packet delivery rate using a low data rate. In this circumstance, the existing passive detection methods [16], which using the LIR value calculated at a single data rate, can't detect the DRDI due to the dynamic rate adaptation. However, an MS with a lower data rate requires more time to transmit a packet than the MSs with higher data rates. Thus, if there is one 'slow' MS contending the wireless channel with some 'fast' MSs, it will induce the well-known performance anomaly problem in 802.11 networks [20], such that the throughput of all the 'fast' mobile stations will degrade as low as the 'slow' one. Therefore, without precisely detecting the DRDI, existing passive interference estimation methods are

unreliable. In this paper, we present AMONET to solve the shortcoming in existing passive interference estimation. This paper makes the following contributions:

- Through extensive measurement studies, we demonstrate that the existing work in passive interference estimation performs poorly in dynamically interfered networks and leads to throughput degradation because it cannot detect the DRDI. To address this problem, we propose AMONET: a passive interference estimation method to detect and mitigate the DRDI.
- We implement the AMONET in QualNet [21] and integrat it to a centralized scheduling system, the Centaur [7]. We compare the improvement in system throughput of Centaur when using the conflict information from AMONET and PIE. The results indicate that AMONET can achieve a system throughput gain of 1.30× and a throughput gain of 2.60× on the victim links, over the Distributed Coordination Function (DCF) while providing better link fairness, in the dense wireless network. In comparison, PIE can achieve a throughput gain of 1.12× and 1.80× over DCF, respectively.

The rest of this paper is organized as follows. In Section II, we discuss related works in passive interference estimation. In Section III, we present the experiment result in a real testbed, which shows the throughput degradation due to the DRDI. And, we present our measurement study to demonstrate the shortcomings in current passive interference estimation. In Section IV, we present the detailed design of AMONET. In Section V, we show a comprehensive evaluation of AMONET by simulation. We conclude our work in Section VI.

II. RELATED WORK

There are many works that focus on interference measurement in the network research community, either active or passive methods. In this section, we briefly survey the related works in the branch of passive interference estimation.

A. Existing approaches in passive interference estimation

Earlier studies in this field, such as Jigsaw [17] and WIT [22] collect off-line data to analyze network performance. WIT analyzes the performance of the IEEE 802.11 MAC protocol using the data traces collected by several sniffers. Similarly, Jigsaw also uses sniffers to collect data traces to study link performance. The most recent study of the passive method is the PIE. PIE is a centralized system which infers the interference relation across the entire Wi-Fi networks using the data traces collected at different APs. A central controller is used to merge the traffic traces and analyze the LIR (will be described in Section 2.2) and packet overlapping relation, then the controller can accurately infer the APs' Carrier Sense and Hidden Terminal relation.

B. The Link Interference Ratio (LIR)

LIR is a widely used metric in current passive interference detection to infer the interference relation between any two links [18], [20]. For a pair of links, LIR is the ratio of the

transmission performance when they transmit simultaneously, to the performance when they transmit individually. Its value ranges from 0 to 1. LIR of 1 indicates the two links do not interfere, whereas, LIR of 0 indicates there is heavy interference between the two links. In practice, a threshold of 0.8 is widely used to judge the existence of interference [18], [20]. Note that, we use the notation L_{AP_i,MS_j} to represent a wireless link from AP_i to MS_j.

LIR can be calculated in both passive and active ways. The active way is the Unicast Bandwidth Test (UBT) [18] which uses the measured throughputs of links when they transmit unicast data. The LIR estimated using UBT is given by:

$$LIR\_UBT_{AP_3MS_4 \to AP_1MS_2} = \frac{U_{AP_3MS_4 \to AP_1MS_2}}{U_{AP_1MS_2}} \quad (1)$$

where $U_{AP_1MS_2}$ is the unicast throughput of L_{AP_1,MS_2} when it transmits individually, and $U_{AP_3MS_4 \to AP_1MS_2}$ is the unicast throughput of L_{AP_1,MS_2} when it transmits simultaneously with L_{AP_3,MS_4}. The LIR_UBT directly shows the decrease of transmission efficiency on L_{AP_1,MS_2} when it transmits together with L_{AP_3,MS_4}. UBT is widely regarded as the reference of interference estimation [17], [18], [20]. However, it requires an overhead of $\mathcal{O}(n^4)$ to estimate the interference relation for an n node network, which is not applicable in practice. According to the experiment result given in [23], the running time of UBT in a 20 nodes topology is more than one hour.

On the other hand, a passive way to calculate the LIR is to use the overlapping packets delivery rate [16], which shows the probability of a wireless link to successfully transmit its packet at a certain data rate when it transmits simultaneously with the potential interferer. The LIR calculated using the Packet Delivery Rate (PDR) is defined as:

$$LIR\_PDR_{AP_3MS_4 \to AP_1MS_2,r} = \frac{R_{AP_3MS_4 \to AP_1MS_2,r}}{R_{AP_1MS_2,r}}$$
$$(2)$$

where $R_{AP_1MS_2,r}$ is the packet delivery rate of L_{AP_1,MS_2} when it transmits individually at the data rate r, and $R_{AP_3MS_4 \to AP_1MS_2,r}$ is the delivery rate of L_{AP_1,MS_2} when it transmits simultaneously with L_{AP_3,MS_4} at the data rate r.

In summary, in addition to detecting the well-studied Carrier Sense and the collision induced interference in the hidden terminal problem, the AMONET is able to detect the Data Rate Degradation which is also caused by the hidden terminal problem.

III. PROBLEM DEFINITION AND MOTIVATION

In this section, we first introduce the types of interference that we are focusing in this paper. After that, we present an experiment in a real testbed to study the DRDI. Then, a measurement study on the interference estimation in a multiple rates environment is presented, in which we analyze the interference detection result of PIE, and demonstrate that the existing passive interference detection methods can't detect the DRDI.

A. Types of interference

In this paper we focus on the interferences among the downlink transmissions, from APs to MSs, because the downlink traffic occupies around 85% of the entire traffic in the Wi-Fi networks [24]. In the downlink case, the interference can be broadly classified into two categories: **1)** the Carrier Sense (CS) interference between two APs, which determines how the APs can share the wireless channel; and **2)** the collision induced interference at the MSs, due to the hidden terminal problem.

For any two APs sharing the same wireless channel, AP_i and AP_j, there are four cases of **CS interference**: **1)** $AP_i \leftrightarrow AP_j$: if AP_i and AP_j can carrier sense the transmission of each other; **2)** $AP_i \leftarrow AP_j$: if AP_j can carrier sense the transmission of AP_i, but AP_i can't sense AP_j; similarly we have **3)** $AP_i \rightarrow AP_j$; **4)** $AP_i \nleftrightarrow AP_j$: if AP_i and AP_j can't carrier sense each other. If at least one of the two APs can't carrier sense the other one, their simultaneous transmissions will cause the collision induced interference on the MSs. This is widely known as the hidden terminal problem. Although the concept of hidden terminal problem is widely used in current literature [13], [15], we still lack of a detailed definition of it in multiple rates scenario, in which APs can still transmit their packets successfully after degrading the data rates, if the interference from the hidden terminal is not severe. Note that a wireless link may degrade its transmission data rate due to various reasons, such as the increase of transmission distance, the channel noise, or the interference from non-Wi-Fi devices. The problem we are focusing in this paper arises from the collision induced interference due to the hidden terminal problem. We define and use the following definitions in this paper:

Definition 1. Hidden Terminal Interference (HTI). If 1) the simultaneous transmission of L_{AP_3,MS_4} causes packets collisions on MS_2 and 2) the Packet Delivery Rate of L_{AP_1,MS_2} is below 0.8 (more than 20% packet loss) even if L_{AP_1,MS_2} has degraded its transmission data rate to the lowest one. Then, we say L_{AP_3,MS_4} causes the HTI on L_{AP_1,MS_2}.

Definition 2. Data Rate Degradation due to Interference (DRDI). If 1) the concurrent transmission of L_{AP_3,MS_4} causes packets collisions on MS_2 but 2) L_{AP_1,MS_2} can still achieve a Packet Delivery Rate over 0.8 by using a lower data rate. Then, we say L_{AP_3,MS_4} causes the DRDI on L_{AP_1,MS_2}.

Both HTI and DRDI can be regarded as the symptoms of the hidden terminal problem, but they will cause different results.

B. Experiments in real testbed

We set up an indoor testbed to investigate the significant throughput degradation caused by the DRDI in a practical Wi-Fi networks. As shown in Fig. 1, the testbed consists of two Cisco WRT610N series APs, AP_1 and AP_2, that have wired connection to the PCs running the Iperf [25]. We have three
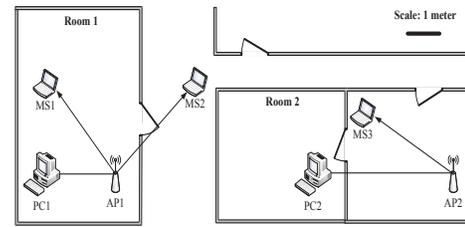

Fig. 1: The topology of the testbed consists of two APs and three mobile stations.
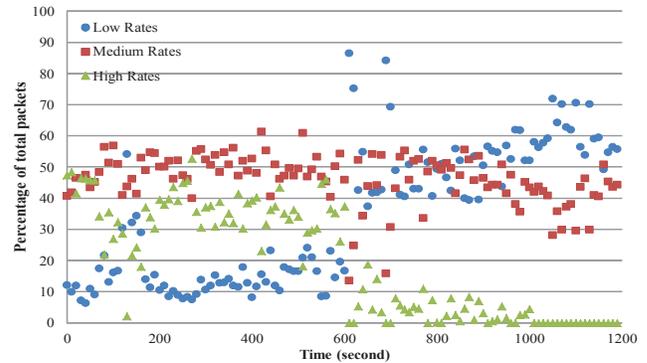

Fig. 2: Percentages of packets transferred from AP_1 to MS_2 at different data rate groups during the 20 minutes experiment.

mobile stations, MS_1 is a laptop with the Realtek RTL8188CE wireless card, MS_2 is a laptop with the Ralink RT3090 card and MS_3 is a laptop using the Intel Dual Band Wireless-AC 7260 wireless card. MS_1 and MS_2 are associated with AP_1 and MS_3 is associated with AP_2. The APs are configured to use the same channel in the 2.5GHz band. Moreover, we fixed the network mode as IEEE 802.11n and used the default auto-rate adaptation algorithm [19] in the APs to support data rate adaptation. In all the experiments we disabled the RTS/CTS handshake and fixed the transmission power to ensure those two APs can't carrier sense each other. We put MS_1 inside Room 1 which was three meters away from AP_1, so that it would not suffer any interference from the transmission of AP_2. On the other hand, we put MS_2 at the corridor between Room 1 and Room 2, and it was also three meters away from AP_1. But the transmission from AP_2 would cause the DRDI on MS_2. We used the Iperf running on both PC_1 and PC_2 to generate the downlink UDP traffic from APs to mobile stations. The offered traffic load was configured as 30 Mbps.

We set up a 20 minutes experiment. In the first 10 minutes, only AP_1 was activated, after that we also activated AP_2, so that the transmission from AP_2 to MS_3 would cause the DRDI on MS_2. During the experiment, we collected the traces of the wireless network traffic and analyzed the adaptation of the data rates. Because of the rate diversity, we simply classify the data rates into three groups: the data rates of 6.5, 13 and 19.5
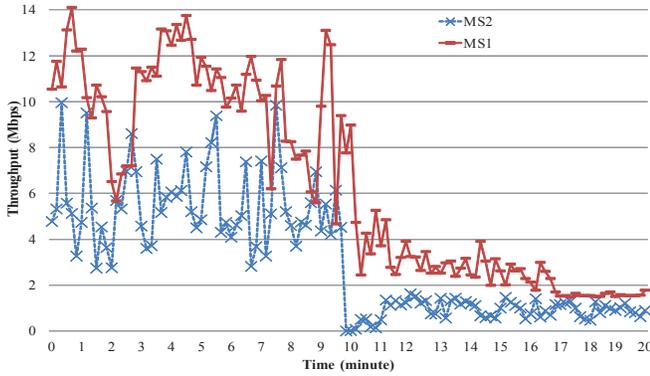
Fig. 3: The throughputs of both MS_1 and MS_2 during the 20 minutes experiment.

Fig. 4: A simple Hidden Terminal topology consists of two 802.11n wireless links.

Mbps serve as the Low Rates group; 26 and 39 Mbps serve as the Medium Rates group; 52 Mbps and higher rates serve as High Rates group. Fig. 2 shows the percentages of packets transferred from AP_1 to MS_2 using each of those three data rate groups during the 20 minutes experiment. We can see that in the first 600 seconds, the percentage of the packets transmitted using 'High' data rates is about 50 percent, and only around 10 percent of packets were transmitted using a 'Low' data rate. However, after 600 seconds, when the DRDI happened, the percentage of High Rates decreased below 10 percent, whereas, the percentage of Low Rate increased and was above 50 percent. This data rate degradation happened on MS_2 caused the performance anomaly problem on MS_1. As shown in Fig. 3, in the first 10 minutes, the throughputs of MS_1 and MS_2 are around 10 Mbps and 6 Mbps, respectively. After 10 minutes, the throughput of MS_2 decreased to 1 Mbps due to the DRDI from AP_2, and the throughput of MS_1 also decreased to 3 Mbps due to the performance anomaly problem caused by the DRDI on MS_2. Thus, it is essential to detect and provide the DRDI information to the upper-layer applications, such as the centralized scheduling system, to resolve the interference. In the next section, we present our measurement study of the existing passive interference estimation method, which shows that the existing method can't accurately detect the DRDI.

C. A measurement study of passive interference estimation in dynamic environments

Previous studies [4], [23] have shown that the interference relation between wireless links is affected by the link's physical data rate. Although previous study on passive interference estimation, PIE, has been proven to be accurate in estimating the LIR_PDRs for different data rates, it only uses the LIR_PDR calculated at a single data rate to judge the interference relation. Without showing how to apply the LIR_PDRs calculated at different data rates to infer the interference relations in multi-rates environment, it may result in a misjudgement of interference relation.
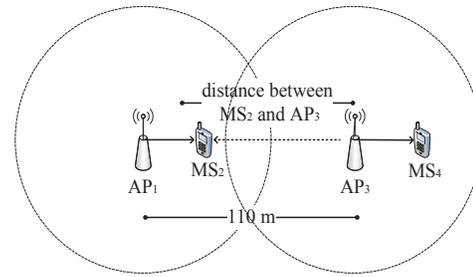
To understand the above problem, we conduct extensive simulations in QualNet using a simple hidden terminal topology shown in Fig. 4. The topology consists of two APs and two MSs sharing the same channel in 802.11n. We use the Two-ray pathloss model and the lognormal shadowing model with 8dB shadowing mean in all the simulations in this paper. The solid lines with arrow represent the association relations between AP and MS, while the dashed line with arrow represents the potential interference relation. Transmission ranges of the APs are configured as 80 meters. The dash circles indicate the carrier sensing ranges of AP_1 and AP_3. The distance between AP_1 and AP_3 is around 110 meters and they can't sense each other. Thus, those two links are in the hidden terminal problem and the transmission of L_{AP_3,MS_4} may cause interference on L_{AP_1,MS_2}. However, according to our previous definitions, depending on the distance between MS_2 and AP_3 and the offered traffic load, it may result in either HTI or DRDI.

We construct a number of scenarios by adjusting the distance from MS_2 to its potential interferer AP_3. We estimate the interference level of L_{AP_3,MS_4} on L_{AP_1,MS_2} for every three meters when the distance changes from 110 meters to 65 meters. In addition, we adjust the offered traffic load on those two links among 3, 6 and 9 Mbps, to take the influence of traffic load into account. Every scenario was simulated more than 20 times by varying the random seed value used in the QualNet, which will affect the feature of both signal propagation and wireless environment. We also disable the Request-to-Send/Clear-to-Send (RTS/CTS) handshake for all the nodes, and apply the Auto Rate Fallback (ARF) implemented in the QualNet to support rate adaptation. We use both unicast throughput and packet delivery rate, defined in Eq. (1) and Eq. (2), to calculate the LIR_UBT and LIR_PDR, respectively. Note that, in case of deciding interference relation, the LIR_Threshold of 0.8 is applied. If the LIR_UBT is less than the LIR_Threshold, the UBT [18] will infer the links are in an interference relationship. Similarly, if the LIR_PDR of the lowest data rate (6.5 Mbps in case of 802.11n, notated as LIR_PDR$_{6.5Mbps}$) is less than LIR_Threshold, PIE will judge them as interference. Like the previous works in the literature [18], [20], we regard the interference relation measured by the UBT as the ground truth.

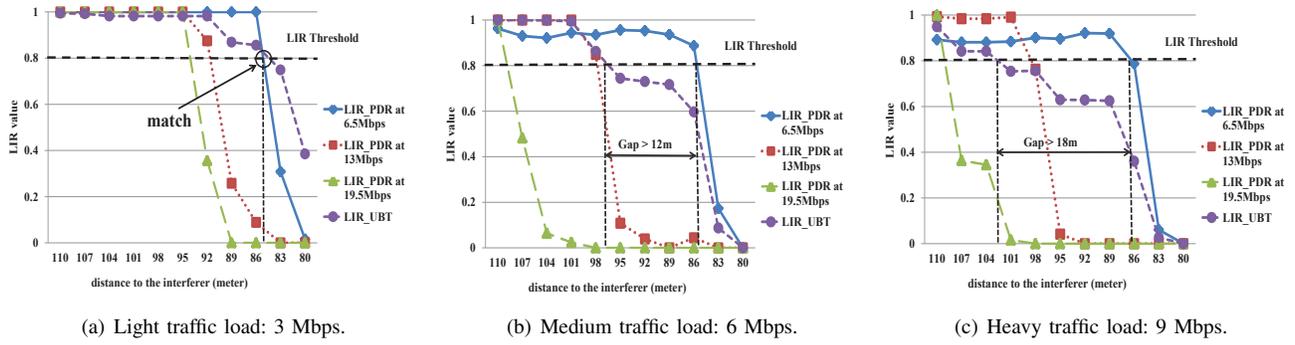Fig. 5 shows the distributions of the LIRs of L_{AP_3,MS_4}

(a) Light traffic load: 3 Mbps.   (b) Medium traffic load: 6 Mbps.   (c) Heavy traffic load: 9 Mbps.

Fig. 5: The LIRs of L_{AP_3,MS_4} on L_{AP_1,MS_2} when MS_2 moves forward to AP_3.
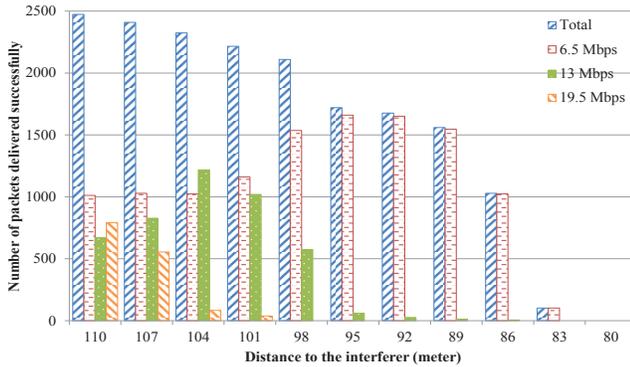

Fig. 6: The number of packets successfully delivered by L_{AP_1,MS_2} at three different data rates (6.5, 13 and 19.5 Mbps) under the interference from L_{AP_3,MS_4} and with a 6 Mbps traffic load.

on L_{AP_1,MS_2}. Three data rates (6.5, 13 and 19.5 Mbps) are used by L_{AP_1,MS_2} during the experiment. Thus, we estimate the LIR_PDR based on the packet delivery rate of L_{AP_1,MS_2} at each of those data rates (following Eq. (2)), denoted as LIR_PDR$_{6.5Mbps}$, LIR_PDR$_{13Mbps}$ and LIR_PDR$_{19.5Mbps}$, respectively. Fig. 5 also shows the LIR_UBT calculated based on the unicast throughput of L_{AP_1,MS_2} (following Eq. (1)). As we expected, when MS_2 moves closer to AP_3, all the three LIR_PDRs and LIR_UBT are decreased. Moreover, the decrease of LIRs (both LIR_PDR and LIR_UBT) start earlier in the case when the offered traffic load is heavy (9 Mbps), than in the cases when traffic load is either light (3 Mbps) or medium (6 Mbps). This is because, with the increase of the offered traffic load, the collision happens more frequently on MS_2. **In case of light traffic load**, shown in Fig. 5(a), the LIR_UBT indicates that L_{AP_1,MS_2} suffers interference from L_{AP_3,MS_4} when the distance between MS_2 and AP_3 is less than 83 meters. Moreover, the LIR_PDR$_{19.5Mbps}$ and LIR_PDR$_{13Mbps}$ decrease below the LIR_Threshold much earlier than LIR_UBT, due to their poor robustness against the interference. However, the value of LIR_PDR$_{6.5Mbps}$ decreases below the LIR_Threshold not until the distance reduces

to 83 meters. In this case, the estimation result of PIE using the LIR_PDR$_{6.5Mbps}$ matches the result of the UBT which we regarded as the reference of interference. Both of them infer the interference on L_{AP_1,MS_2} starts when the distance is less than 83 meters. **In case of medium traffic load**, shown in Fig. 5(b), with the increasing of the traffic load, more collisions happen at MS_2. Thus, the LIR_UBT shows that L_{AP_3,MS_4} will cause heavy interference on L_{AP_1,MS_2} from a position much earlier than that in the light traffic load case. From Fig. 5(b), we can see that the LIR_UBT drops below the LIR_Threshold when the distance is around 95 meters. However, LIR_PDR$_{6.5Mbps}$ still maintains above the LIR_Threshold until the distance decreases to 83 meters. The UBT estimates that L_{AP_1,MS_2} suffers interference from L_{AP_3,MS_4} when the distance is 95 meters, whereas, the PIE shows the interference starts from 83 meters, which is a 12 meters difference. Thus, there is a gap area in which the estimation results of the UBT and PIE are different. **In case of heavy traffic load**, as shown in Fig. 5(c), the result is similar to that in the medium traffic load. We can notice that the LIR_UBT drops below the LIR_Threshold when the distance is around 101 meters. But, the value of LIR_PDR$_{6.5Mbps}$ can maintain above the LIR_Threshold until the distance is smaller than 83 meters. In this case, the range of the gap area increases to 18 meters.

An interesting question is: *what causes the gap between the estimation results between the UBT and PIE? And what happens on the link L_{AP_1,MS_2} within the gap area?*

To answer the above question, let's analyze the gap area shown in Fig. 5(b) and the measurement result of L_{AP_1,MS_2} shown in Fig. 6, which shows the number of successful packets delivered at each of the data rates that L_{AP_1,MS_2} used. In Fig. 5(b), the gap area starts from 95 meters to 83 meters: the LIR_UBT drops below the LIR_Threshold when the distance is around 95 meters, whereas, the LIR_PDR$_{6.5Mbps}$ drops below the LIR_Threshold not until 83 meters. Fig. 6 shows that the total number of successful packets drops dramatically when the distance decreases from 98 meters to 95 meters. Moreover, when the distance is between 95 meters and 86 meters (the gap area), nearly all the successful packets are sent at the data rate of 6.5 Mbps. Again, this is because AP_1 de-
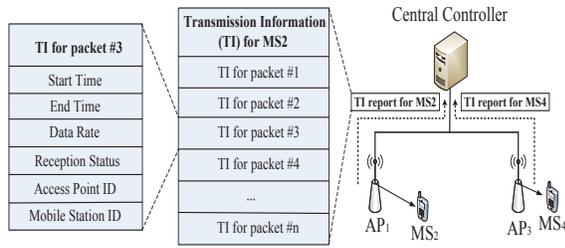

Fig. 7: An example of the AMONET architecture which consists of a central controller, two APs and two MSs.

grades its transmission data rate to resist the interference from L_{AP_3,MS_4}. According to the distribution of LIR_PDR$_{6.5Mbps}$ shown in Fig. 5(b), L_{AP_1,MS_2} can still achieve a high packets delivery rate at 6.5 Mbps until the distance reaches 83 meters. However, due to the decrease of total successful packets and the degradation of transmission data rate, the throughput of link L_{AP_1,MS_2} decreases dramatically within the gap area, as the LIR_UBT indicates in Fig. 5(b). The interference L_{AP_3,MS_4} on L_{AP_1,MS_2} within the gap area is the DRDI which we defined previously. Lastly, when the distance is smaller than 83 meters, even the lowest data rate can't resist the interference, both the LIR_UBT and LIR_PDR$_{6.5Mbps}$ decrease to 0. From Fig. 6, we can notice that nearly no packets can be received at MS_2 when the distance is smaller than 83 meters. In this case, the interference L_{AP_3,MS_4} on L_{AP_1,MS_2} is the HTI. Note that, using the LIR_PDR at a single rate in PIE can detect the HTI but fails to detect the DRDI. Because the DRDI happens in the gap area as shown in Fig. 5, in which the LIR_PDR$_{6.5Mbps}$ is still above the LIR_Threshold. On the other hand, though the UBT can clearly detect both the HTI and DRDI using the LIR_UBT, it is not applicable in practice due to its large computing overhead, as mentioned before.

IV. THE DESIGN OF AMONET

In this section, we present the design of AMONET. We outline the architecture of AMONET and introduce the algorithms to detect the Carrier Sense, HTI, and DRDI.

A. System overview

Following the trend in the existing passive interference estimation, AMONET is a centralized system consisting of a central controller, and with all the APs connected to the controller through wired networks, where the main function of interference estimation is implemented. The APs are required to record the Transmission Information (TI) for every packet they have transmitted. The information includes: **1)** an accurate timestamp showing the start time and end time of the packet; **2)** the data rate the packet has been transmitted; **3)** the reception status showing if the packet has been successfully delivered; and **4)** the IDs of the AP (source) and MS (destination). As an example shown in Fig. 7, for every packet AP_1 sends to MS_2, AP_1 creates a timestamp for that packet

and records the data rate it used for transmission. In order to achieve this, AMONET requires a slightly modification on the APs. After receiving the corresponding ACK from MS_2, AP_1 will update the packet's reception status. APs will report the collected TIs to a central controller periodically. The length of the report period can be configured empirically. While a short period can ensure a lower computation overhead and faster update, a long period can enable higher detection accuracy. In our setting, the report period is configured as three seconds, which ensures both low computation overhead and high detection accuracy.

B. Detection of the Carrier Sense (CS) interference

Corresponding to each of the four Carrier Sense relations we introduced in Section 3, for any two APs, AP_i and AP_j, their packet transmissions can have four kinds of **overlapping relation**: **1) Non-Overlapping**: if their CS relation is $AP_i \leftrightarrow AP_j$, according to the IEEE 802.11 CSMA/CA mechanism, both of the two APs will defer their transmissions to avoid packet collisions whenever they sense the other AP is sending packets. Thus, the controller will not find any overlapped packet between those two APs; **2) One-way-Overlapping**: in case of $AP_i \leftarrow AP_j$, the controller can observe that the packets from AP_i overlap with the packets from AP_j. Because AP_i will keep sending its packets even if AP_j is using the channel. However, AP_j will defer its transmission while AP_i is occupying the channel. Similarly, we have the relation $AP_i \rightarrow AP_j$; **3) Two-way-Overlapping**: if $AP_i \nleftrightarrow AP_j$, neither AP_i nor AP_j will not defer its transmission even if the other AP is sending, thus the controller will observe their packets overlap with each other.

To infer the CS interference, the controller will merge and sort the collected TIs in the order of the transmission start-time based on the same timeline. Note that, this requires the times at both the APs and controller are synchronized, which can be achieved using the Precision Time Protocol [26]. After sorting, the controller analyzes the overlapping relation between the APs' packet transmissions. Then, based on the packets overlapping relationship, the controller can infer the APs' Carrier Sense relation.

The details are shown in **Algorithm 1**. The controller takes merged and sorted TI list, $LIST_{TI}$, as the input and analyze their overlapping relation. In order to check the overlapping relation of two TIs from two different APs, TI_i and TI_j, the controller compares their timestamps. If the start-time of TI_i (denoted as TS_i) is later than the start-time of TI_j (TS_j), but earlier than TI_i's end-time (TE_i), we infer that TI_j overlaps with TI_i. On the other hand, if $TS_j < TS_i < TE_j$, we can infer that TI_i overlaps with TI_j. For every two TIs in the $LIST_{TI}$, the controller analyzes their overlapping relation and records the overlapping times into the result set, $LIST_{overlap}$. Then, using the records in the $LIST_{overlap}$, the controller can judge the CS relation between two APs, AP_i and AP_j. As recorded in $LIST_{overlap}$, if the number of packets from AP_i overlapped the packets from AP_j is more than the threshold δ (equals to 50 in our configuration to assure the accuracy),

Algorithm 1 Detection of the Carrier Sense (CS) Interference

Require: 1) $LIST_{TI}$; **2)** $LIST_{AP}$.
Ensure: 1) CS_Result; **2)** $LIST_{overlap}$.
1: **function** CSRELATION($LIST_{TI}, LIST_{AP}$)
2:     $LIST_{overlap} \leftarrow empty$, $CS\_Result \leftarrow empty$
3:     **for any** TI_i and TI_j **in** $LIST_{TI}$ **do**
4:         **if** $TI_i.AP_{ID} \neq TI_j.AP_{ID}$ **then**
5:             CHECKOVERLAP($TI_i, TI_j, LIST_{overlap}$)
6:     **for any** AP_i and AP_j **in** $LIST_{AP}$ **do**
7:         **if** $!LIST_{overlap}.Time(AP_i, AP_j) > \delta$ **then**
8:             $CS\_Result.Add(AP_i, AP_j)$
9:     **return** CS_Result

---

then the controller infers that AP_i can't carrier sense AP_j, otherwise, AP_i can carrier sense AP_j. Finally, the detection result of CS relation is recorded in the result set, CS_Result.

C. Detection of the HTI and the DRDI

The prerequisite for any two links in the HTI or DRDI relation is that at least one of APs can't carrier sense the other one. Therefore, to detect the links' interference relation, the controller gets the Carrier Sense relations between all the APs, CS_Result, from **Algorithm 1**. The pseudo code for detecting the HTI and DRDI is given in **Algorithm 2**. The controller maintains a list which stores the information for all the links, $LIST_{link}$. For any two links in $LIST_{link}$, $Link_i$ and $Link_j$, the controller checks APs' Carrier Sense relation by using CS_Result. If their APs can't carrier sense each other, the controller will analyze their interference relation based on LIR_PDR. The algorithm for calculating the links' LIR_PDR is given in **Algorithm 3**.

Based on Eq. (2), for two links, $Link_i$ and $Link_j$, $LIR\_PDR_{i \to j,r}$ shows the performance loss on $Link_j$ when it transmits at data rate r simultaneously with $Link_i$. As shown in **Algorithm 3**, $R_{i \to j,r}$ indicates the packet delivery rate of $Link_j$ at rate r when transmitting together with $Link_i$. To calculate $R_{i \to j,r}$, the controller measures the overlapping information between those two links. The value of $O_{i \to j,r}$ is the number of packets from $Link_j$ transmitted at rate r overlapped by the packets from $Link_i$. Correspondingly, $OL_{i \to j,r}$ is the number of overlapping packet loss at $Link_j$ when overlap with the transmission from $Link_i$. Similarly, the controller can measure the $R_{j,r}$, which is the packet delivery rate of $Link_j$ at rate r when transmitting without $Link_i$. $I_{j,r}$ is the number of packet from $Link_j$ transmitted at rate r isolated with the transmission from $Link_i$. Accordingly, $IL_{j,r}$ is the number of packet lost among those isolated transmission. Then, based on $R_{i \to j,r}$ and $R_{j,r}$ we can get $LIR\_PDR_{i \to j,r}$. The controller will repeatedly calculate $LIR\_PDR_{i \to j,r}$ for every data rate r used by $Link_j$ lately. LIR_PDR will be used in **Algorithm 2** to compute the interference relation between two links.

Similar with PIE, the accuracy of AMONET in interference detection is affected by the network scale and transmission diversity. In a large network consisting of multiple interferers,

Algorithm 2 Detection of the HTI and DRDI

Require: 1) $LIST_{Link}$; **2)** $LIST_{overlap}$; **3)** CS_Result.
Ensure: $Interference\_Result$.
1: **function** DETECTIONIR($LIST_{Link}$)
2:     **for any** $Link_i$ and $Link_j$ **in** $LIST_{Link}$ **do**
3:         $AP_i \leftarrow Link_i.AP$, $AP_j \leftarrow Link_j.AP$,
4:         **if** $!CS\_Result.Has(AP_i, AP_j)$ **then**
5:             $Relation_{i \to j} \leftarrow$ COMPUTEIR($Link_i, Link_j$)
6:             $Interfernce\_Result.Add(Relation_{i \to j})$
7:     **return** $Interfernce\_Result$
8: **function** COMPUTEIR($Link_i, Link_j$)
9:     $LIR\_PDR_{i \to j} \leftarrow$ COMPUTELIR($Link_i, Link_j$)
10:     /*ComputeLIR is given in Algorithm 3*/
11:     **if** $LIR\_PDR_{i \to j}[0] < Threshold$ **then** HTI
12:     **if** $LIR\_PDR_{i \to j}[1] < Threshold$ **then** $DRDI$
13:     **if** $LIR\_PDR_{i \to j}[2] < Threshold$ **then** $DRDI$

Algorithm 3 Calculate the LIR

Require: 1) $LIST_{Link}$; **2)** $LIST_{overlap}$; **3)** CS_Result.
Ensure: $LIR\_PDR_{i \to j}$.
1: **function** COMPUTELIR($Link_i, Link_j$)
2:     $Overlap_{i \to j} = LIST_{overlap}.Get(Link_i, Link_j)$
3:     **for any** r **in** $Overlap_{i \to j}.Rate()$ **do**
4:         $R_{j,r} \leftarrow 1 - IL_{j,r}/I_{j,r}$
5:         $R_{i \to j,r} \leftarrow 1 - OL_{j,i,r}/O_{j,i,r}$
6:         $LIR\_PDR_{i \to j}[r] = R_{i \to j,r}/R_{j,r}$
7:     **return** $LIR\_PDR_{i \to j}$

---

the accuracy of validating the interferer depends on a high transmission diversity. In order to identify the actual interferer from a group of potential interferers, AMONET needs to calculate the exact packet delivery rates of the victim link when transmitting together and isolated with each of the potential interferers, which assumes that the transmission of different links should not highly overlapped. AMONET is able to identify the actual interferer when the transmission overlaps between two links are less than 60%. In practice, the measurement result [17] achieved in a real WLAN shows that around 90% of the wireless transmissions overlap less than 20% of the time. This transmission diversity enables AMONET to be accurate in the real environment.

V. EVALUATION OF AMONET

In this section, we conducted extensive simulations in the QualNet simulator in order to provide that the interference information provided by AMONET can benefit the centralized scheduling algorithm more than previous works.

A. Experimental setup

We compare AMONET with the PIE and integrate both of them to the centralized scheduling algorithm, Centaur [7]. Using the conflict information provided by either AMONET or PIE, Centaur can avoid the downlink interference by allocating conflicted links to non-overlapping time slots, and thus improve the aggregate throughput. Different from AMONET, PIE can't detect the DRDI. Thus, the system throughput of Centaur will decrease due to the performance anomaly
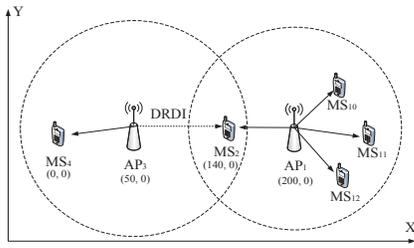
Fig. 8: A two-APs scenario consists of five wireless links. The distance between two APs is 150 meters, and the distance between AP_3 and MS_2 is 90 meters.
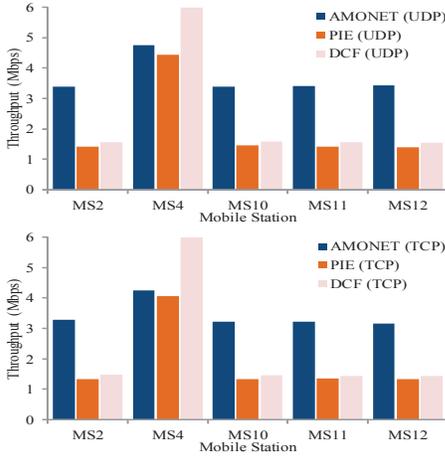

Fig. 9: The throughput of the mobile stations in the Two-APs topology with 6 Mbps traffic load.

problem induced by the DRDI. We evaluate the performance of AMONET in both simple and complex scenarios. First, we use a simple scenario to show the DRDI can cause the aggregate throughput decrease. Second, we use a more complex scenario includes both HTI and DRDI. We evaluate the performance of all scenarios in terms of the aggregate throughput and fairness. The well-known Jain's fairness index [27] is used to evaluate the fairness, the fairness index with a value of 1 indicates the system is 100% fair, whereas, a value of 0 indicates unfairness.

Note that, in all scenarios, we employ IEEE 802.11n and enable the ARF and with RTS/CTS disabled. We assume the APs have the same transmission range and are configured to send saturated traffic to their MSs. Both TCP and UDP traffic are used in all scenarios, with the packet size fixed at 1,400 bytes. The experiments are repeated more than 25 times using different random seeds in the QualNet, that will affect the characteristics of the traffic and wireless environment.

B. Simple scenario: two-APs topology with the DRDI only

In this section, we construct a simple two-APs scenario which only includes the DRDI. We evaluate the performance using both UDP and TCP traffic, with a 6 Mbps traffic load for each mobile station. As shown in Fig. 8, AP_1 and AP_3
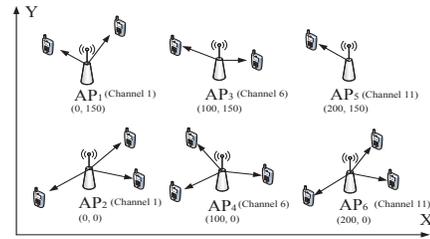

Fig. 10: A complex scenario consists of 6 APs and 14 MSs.

TABLE I: Normalized system throughput gains of Centaur integrate with AMONET and PIE over DCF and the system fairness.

Traffic	Method	Gains	Fairness Index
UDP	AMONET	1.30×	0.91
UDP	PIE	1.12×	0.86
TCP	AMONET	1.28×	0.91
TCP	PIE	1.12×	0.85

can't carrier sense each other, and the transmission from AP_3 will cause the DRDI on link L_{AP_1,MS_2}.

Simulation results. Fig. 9 shows the throughput for each of the MSs, due to the DRDI caused by the interference from link L_{AP_3,MS_4} on link L_{AP_1,MS_2}, the throughput of MS_2 is less than 2 Mbps. Moreover, the performance anomaly problem induced by the rate degradation affected all the other three MSs that associate to AP_1, and made the throughputs of those MSs are as low as that of MS_2. In case of Centaur integrated with PIE (PIE-Centaur), because PIE can't detect the DRDI, Centaur performs no better than DCF. On the other hand, when integrated with AMONET, Centaur can allocate different time slots to the transmissions of L_{AP_3,MS_4} and L_{AP_1,MS_2}, which mitigates the interference occurs on MS_2. As a result, L_{AP_1,MS_2} will be free from the DRDI from L_{AP_3,MS_4}, and thus, will increase the throughput on all the other MSs.

C. Complex scenario: multi-APs topology with both HTI and DRDI

In this subsection, we evaluate AMONET in a complex scenario which includes both HTI and DRDI. As shown in Fig. 11, our topology consists of six APs and their positions are denoted as (x, y). Besides, every two adjacent APs use one of the three orthogonal channels (Channel 1, 6 and 11) in 2.4 GHz, and with a distance of 100 or 150 meters, so that they are out of the carrier sensing range of each other. We distribute 14 MSs and associate them to each of the APs, as shown in Fig. 10, each of the APs may have one to three MSs. Note that, in each of the scenarios we used, the ratio of links suffering either the HTI or DRDI is about 25%, which means around four links among those 14 links are suffering one of those two interferences. This ratio matches the measurement result presented in [16], that about 10% to 30% of links in a Wi-Fi network suffering those two interferences.

Simulation results. Table 2 shows the throughput gains of Centaur over DCF for the complex scenario, when using

TABLE II: Aggregate throughput gains of Centaur with AMONET and PIE on the interfered wireless links over DCF.

Traffic	Mechanism	Gains
UDP	AMONET	2.68×
UDP	PIE	1.80×
TCP	AMONET	2.59×
TCP	PIE	1.82×

the interference information generated by AMONET and PIE, respectively. Because the scenario consists of both HTI and DRDI, the conflict graph created by PIE is not accurate enough to help Centaur to avoid the DRDI. However, comparing with DCF, PIE-Centaur can improve the aggregate throughput by avoiding the HTI and achieve a throughput gain of 1.12× over DCF. On the other hand, using the HTI and DRDI information provided by AMONET, Centaur can effectively resolve both of those conflicts by allocating the conflicted transmissions into different transmission timeslots. As shown in the results, AMONET-Centaur can achieve a throughput gain of 1.30× over DCF. Table 3 shows the aggregate throughput gains of Centaur on the interfered links. The results indicate that, with AMONET, Centaur can achieve a throughput gain more than 2.50 on those interfered AP-to-MS links over DCF, while with PIE, Centaur can only achieve a 1.80 gain over the DCF. This clearly shows that Centaur can largely increase the throughput of the interfered links by using AMONET. In addition, in all the cases, Centaur can achieve better fairness when using AMONET, compare with PIE and DCF.

VI. CONCLUSION AND FUTURE WORK

In this paper, we presented a detailed measurement study of the passive interference estimation in multi-rate Wi-Fi networks. We found that the existing works are not able to detect the DRDI, which will cause dramatic throughput degradation. To address this problem, we presented the AMONET and integrated it with a centralized scheduling system to detect and mitigate the interferences. The results showed that AMONET can greatly benefit the centralized scheduling system and achieved higher throughput than the previous works in interference estimation. As a part of our future work, we will implement our AMONET system in real testbed to evaluate its performance and accuracy in interference detection.

VII. ACKNOWLEDGMENTS

REFERENCES

[1] Cisco, "The zettabyte era: trends and analsis," 2015.

[2] M. A. Ergin, K. Ramachandran, and M. Gruteser, "Understanding the effect of access point density on wireless lan performance," in *Proceedings of ACM MobiCom*, 2007, pp. 350–353.

[3] V. P. Mhatre, K. Papagiannaki, and F. Baccelli, "Interference mitigation through power control in high density 802.11 wlans," in *Procceedings of IEEE INFOCOM*, 2007, pp. 535–543.

[4] J. Huang, G. Xing, and G. Zhou, "Unleashing exposed terminals in enterprise wlans: A rate adaptation approach," in *Proceedings of IEEE INFOCOM*, 2014, pp. 2481–2489.

[5] A. Mishra, V. Brik, S. Banerjee, A. Srinivasan, and W. Arbaugh, "A client-driven approach for channel management in wireless lans," in *Proceedings of IEEE INFOCOM*, 2006, pp. 1–12.

[6] E. Rozner, Y. Mehta, A. Akella, and L. Qiu, "Traffic-aware channel assignment in enterprise wireless lans," in *Proceedings of IEEE ICNP*, 2007, pp. 133–143.

[7] V. Shrivastava, N. Ahmed, S. Rayanchu, S. Banerjee, S. Keshav, K. Papagiannaki, and A. Mishra, "Centaur: realizing the full potential of centralized wlans through a hybrid data path," in *Proceedings of ACM MobiCom*, 2009, pp. 297–308.

[8] J. Manweiler, N. Santhapuri, S. Sen, R. R. Choudhury, S. Nelakuditi, and K. Munagala, "Order matters: transmission reordering in wireless networks," *Networking, IEEE/ACM Transactions on*, vol. 20, no. 2, pp. 353–366, 2012.

[9] W. Zhou, D. Li, K. Srinivasan, and P. Sinha, "Domino: relative scheduling in enterprise wireless lans," in *Proceedings of ACM CoNEXT*, 2013, pp. 381–392.

[10] D. S. Chan, T. Berger, and L. Tong, "Carrier sense multiple access communications on multipacket reception channels: theory and applications to ieee 802.11 wireless networks," *Communications, IEEE Transactions on*, vol. 61, no. 1, pp. 266–278, 2013.

[11] F. Babich, M. Comisso, A. Crismani, and A. Dorni, "On the design of mac protocols for multi-packet communication in ieee 802.11 heterogeneous networks using adaptive antenna arrays," *Mobile Computing, IEEE Transactions on*, vol. 14, no. 11, pp. 2332–2348, 2015.

[12] K. C.-J. Lin, S. Gollakota, and D. Katabi, "Random access heterogeneous mimo networks," *ACM SIGCOMM Computer Communication Review*, vol. 41, no. 4, pp. 146–157, 2011.

[13] K. Jain, J. Padhye, V. N. Padmanabhan, and L. Qiu, "Impact of interference on multi-hop wireless network performance," *Wireless networks*, vol. 11, no. 4, pp. 471–487, 2005.

[14] D. Niculescu, "Interference map for 802.11 networks," in *Proceedings of ACM IMC*, 2007, pp. 339–350.

[15] N. Ahmed and S. Keshav, "Smarta: a self-managing architecture for thin access points," in *Proceedings of ACM CoNEXT*, 2006, p. 9.

[16] V. Shrivastava, S. Rayanchu, S. Banerjee, and K. Papagiannaki, "Pie in the sky: online passive interference estimation for enterprise wlans," in *Proceedings of USENIX NSDI*. USENIX Association, 2011, pp. 337–350.

[17] Y. C. Cheng, J. Bellardo, P. Benkö, A. C. Snoeren, G. M. Voelker, and S. Savage, "Jigsaw," *ACM SIGCOMM Computer Communication Review*, vol. 36, no. 4, pp. 39–50, 2006.

[18] J. Padhye, S. Agarwal, V. N. Padmanabhan, L. Qiu, A. Rao, and B. Zill, "Estimation of link interference in static multi-hop wireless networks," in *Proceedings of ACM IMC*. USENIX Association, 2005, pp. 28–28.

[19] D. Halperin, W. Hu, A. Sheth, and D. Wetherall, "Predictable 802.11 packet delivery from wireless channel measurements," *ACM SIGCOMM Computer Communication Review*, vol. 41, no. 4, pp. 159–170, 2011.

[20] M. Heusse, F. Rousseau, G. Berger-Sabbatel, and A. Duda, "Performance anomaly of 802.11 b," in *Proceedings of IEEE INFOCOM*, vol. 2, 2003, pp. 836–843.

[21] QualNet, http://web.scalable-networks.com/.

[22] R. Mahajan, M. Rodrig, D. Wetherall, and J. Zahorjan, "Analyzing the mac-level behavior of wireless networks in the wild," in *ACM SIGCOMM Computer Communication Review*, vol. 36, no. 4. ACM, 2006, pp. 75–86.

[23] N. Ahmed, U. Ismail, S. Keshav, and K. Papagiannaki, "Measuring multi-parameter conflict graphs for 802.11 networks," *ACM SIGMOBILE Mobile Computing and Communications Review*, vol. 13, no. 3, pp. 54–57, 2010.

[24] J. Eriksson, S. Agarwal, P. Bahl, and J. Padhye, "Feasibility study of mesh networks for all-wireless offices," in *Proceedings of ACM MobiSys*, 2006, pp. 69–82.

[25] Iperf, http://iperf.fr.

[26] D. L. Mills, "Internet time synchronization: the network time protocol," *Communications, IEEE Transactions on*, vol. 39, no. 10, pp. 1482–1493, 1991.

[27] R. Jain, D.-M. Chiu, and W. R. Hawe, *A quantitative measure of fairness and discrimination for resource allocation in shared computer system*. Eastern Research Laboratory, Digital Equipment Corporation Hudson, MA, 1984, vol. 38.